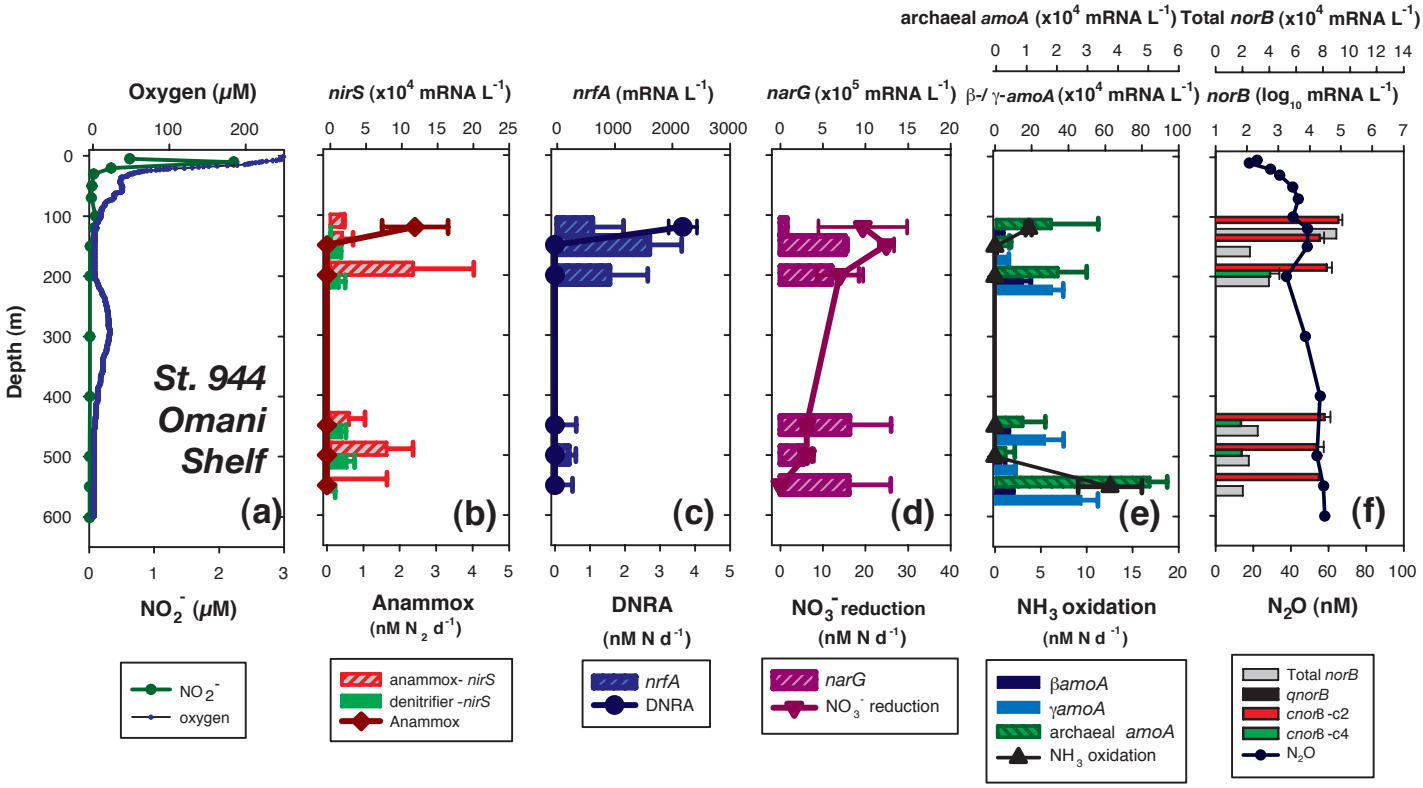

Figure A1. Vertical distribution of (a) oxygen and nitrite concentrations over the Omani Shelf, along with measured N-transformation rates and the corresponding functional gene expression levels: (b) anammox rates, anammox- and denitrifier- *nirS* expression, (c) DNRA rates and *nrfA* expression, (d) nitrate reduction and *narG* expression, (e) ammonium oxidation rates, archaeal and bacterial *amoA* expressions, (f) N_2O and various forms of *norB* expressions.

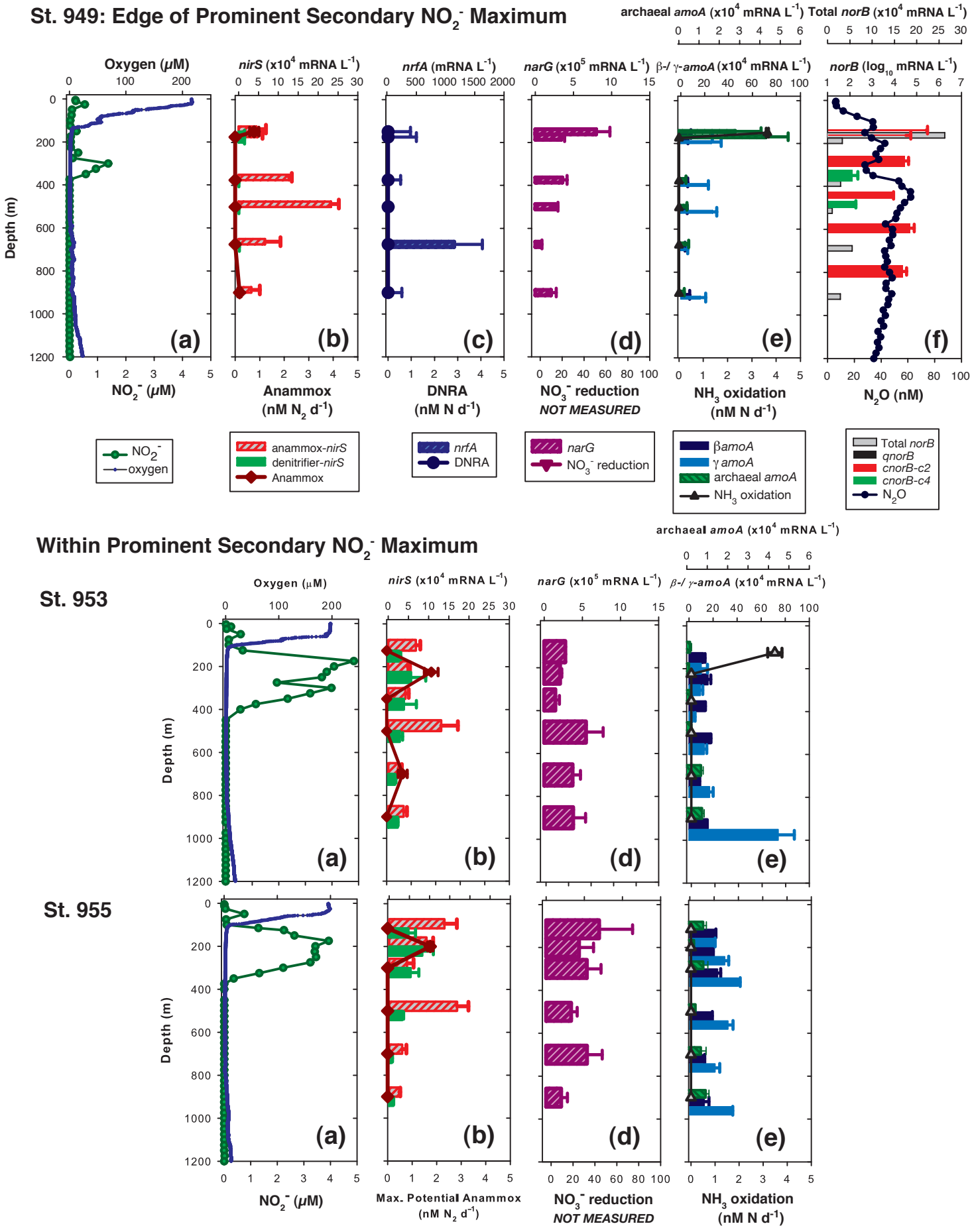

Figure A2. Vertical distribution of various chemical properties, N-transformation rates and the corresponding functional gene expressions at Sts. 949 (top), 953 (middle) and 955 (bottom) in the central northeastern Arabian Sea OMZ: (a) oxygen and nitrite concentrations, (b) anammox rates, anammox- and denitrifier- *nirS* expression, (c) DNRA rates and *nrfA* expression, (d) nitrate reduction and *narG* expression, (e) ammonium oxidation rates, archaeal and bacterial *amoA* expressions, (f) N_2O and various forms of *norB* expressions.

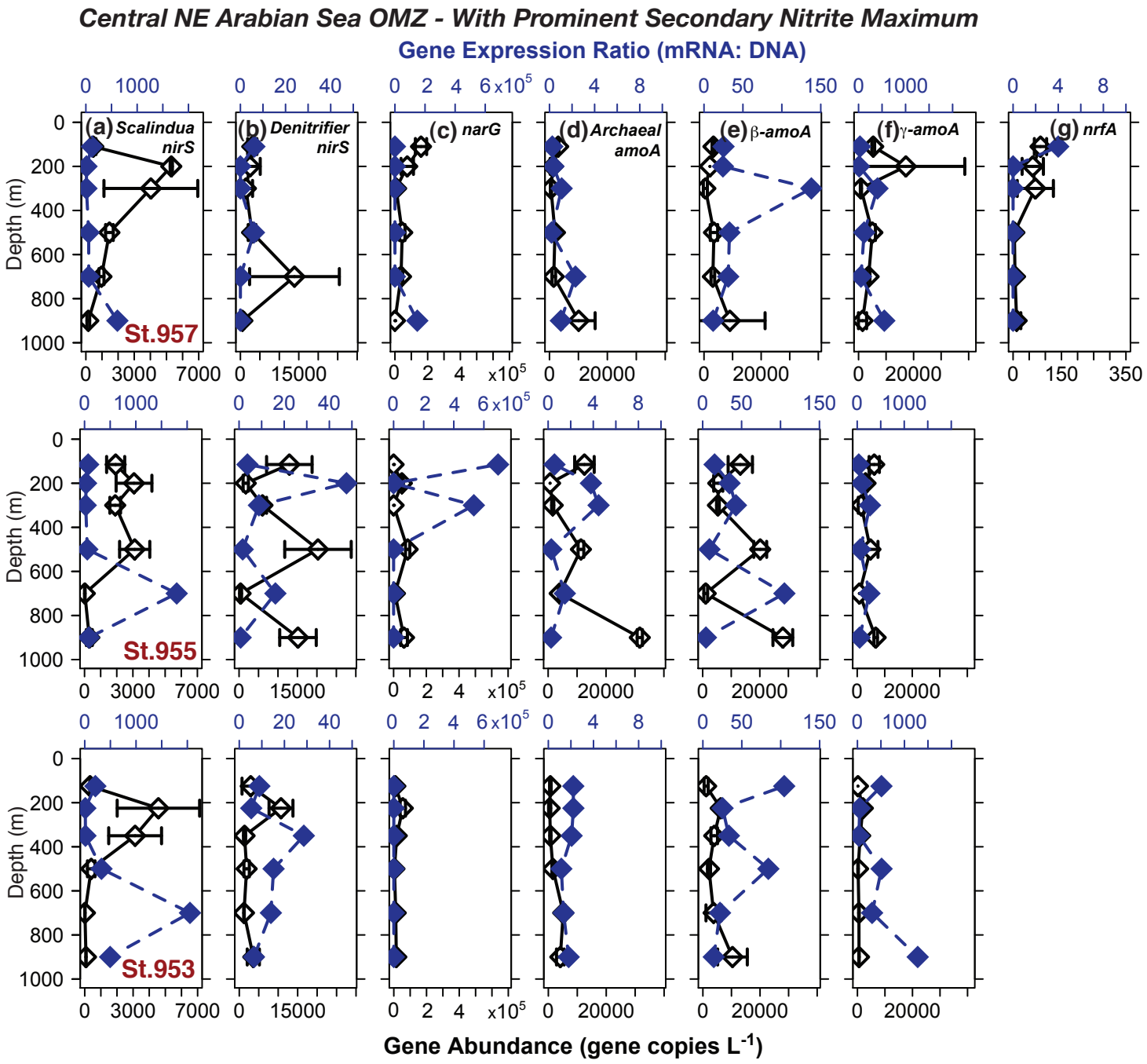

Figure A3. Vertical distribution of gene abundance (black open symbols) and gene expression ratios (mRNA: DNA) (blue solid diamonds) at three stations (top: St. 957, middle: St. 955, bottom: St. 953) in the central northeastern Arabian Sea OMZ that was characterized by prominent secondary nitrite maxima: (a) anammox (Scalindua- specific) *nirS* gene, (b) denitrifier *nirS* genes, (c) *narG* genes, (d) archaeal *amoA* genes, (e) β-proteobacterial *amoA* genes, (f) γ-proteobacterial *amoA* genes and (g) *nrfA* genes.

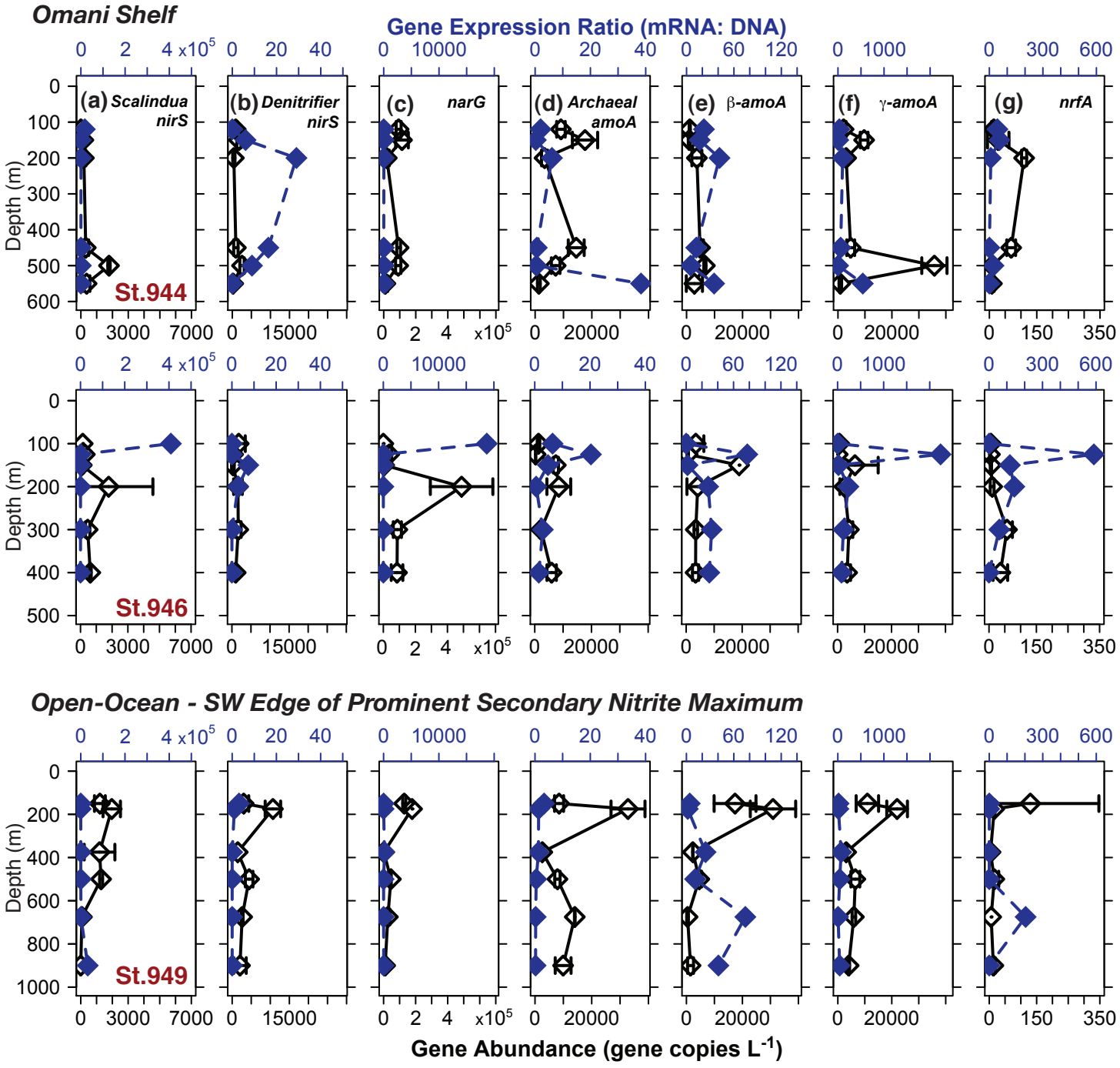

Figure A4. Vertical distribution of gene abundance (black open symbols) and gene expression ratios (mRNA: DNA) (blue solid diamonds) in the OMZ water column over the Omani Shelf (top two rows) and in the open ocean at the southwestern edge of the prominent secondary nitrite maximum: (a) anammox (Scalindua- specific) *nirS* gene, (b) denitrifier *nirS* genes, (c) *narG* genes, (d) archaeal *amoA* genes, (e) β-proteobacterial *amoA* genes, (f) γ-proteobacterial *amoA* genes and (g) *nrfA* genes.

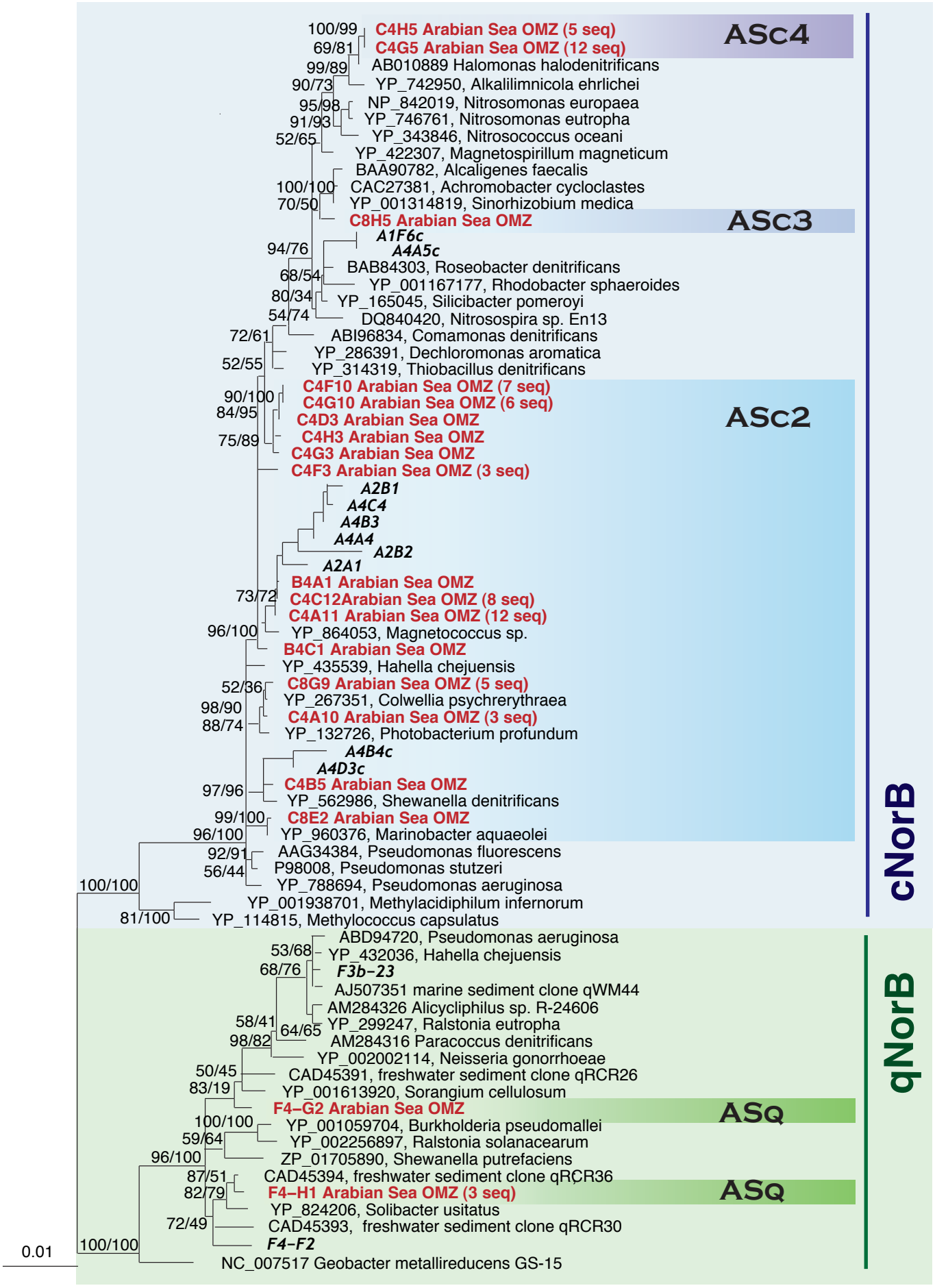

Figure A5. A phylogenetic recontruction of quinol- and cytochrome *c*- containing nitric oxide reductase subunit B (qNorB and cNorB respectively) based on deduced amino acid sequences obtained in the Arabian Sea OMZ (bold) in this study. Shown here is the best maximum likelihood (ML) tree after 100 resamplings (bootstrap values of ML/ maximum parsimony, MP, are shown), and its topology is supported by both MP and distance matrix methods. Only sequences of ≥190 amino acids long were used in tree construction, while sequences in italics were shorter and added afterwards based on MP, if gene sequences had <99% sequence identity as representatives already shown. Highlighted in boxes are sequences targeted by quantitative PCR with specifically designed primers and probes. Branch lengths are in sequence divergence.

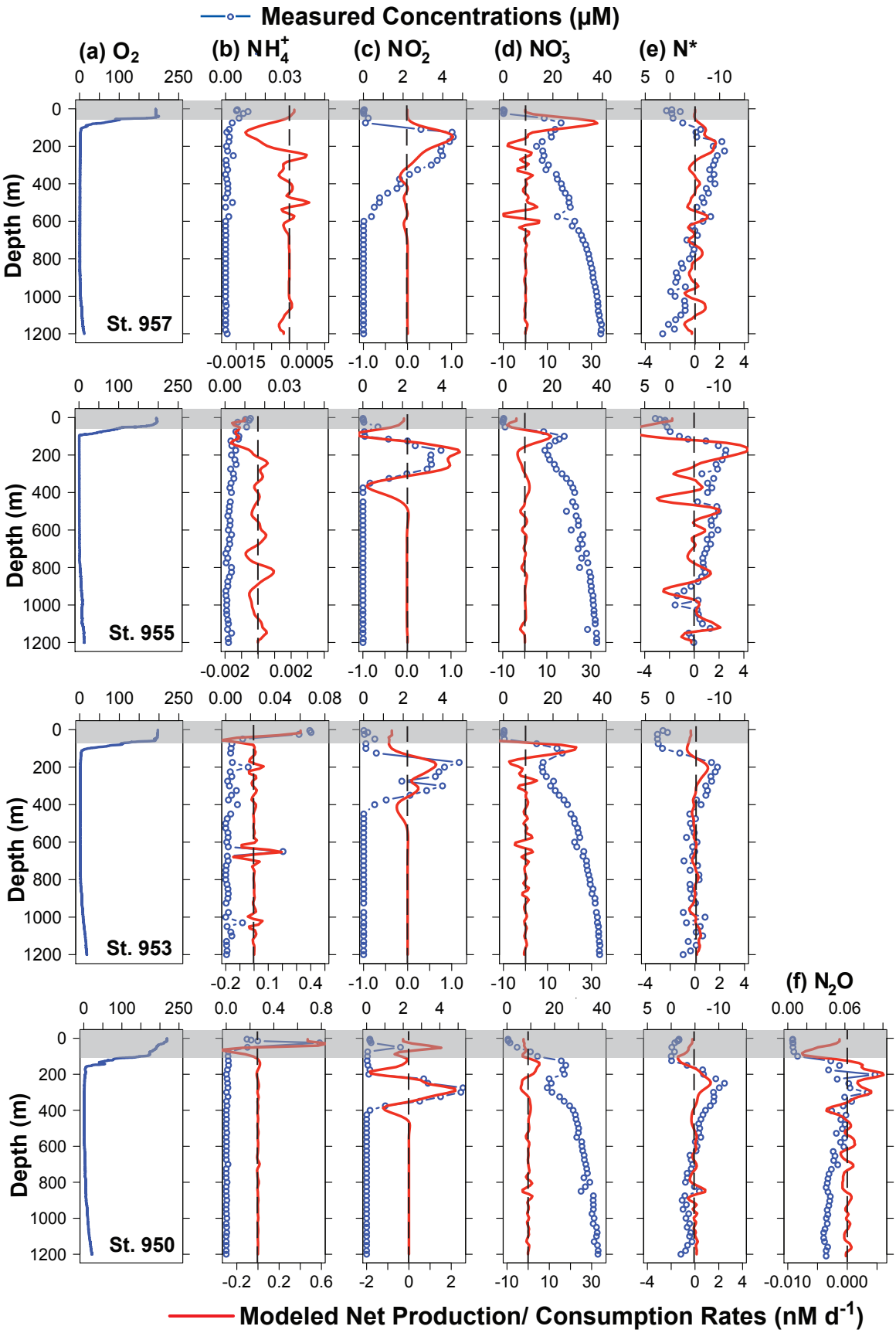

Figure A6. (a) Vertical distribution of oxygen at the four open-ocean Arabian Sea stations within the zone of prominent secondary nitrite maxima (>0.2 µM) in the OMZ, along with the corresponding profiles of measured concentrations of inorganic nitrogen, based on which net production (positive) or consumption (negative) rates were modeled: (b) NH_4^+, (c) NO_2^-, (d) NO_3^-, (e) N* and (f) N_2O. In case of (e) N*, positive rates reflect production of more severe N-deficits (i.e. more negative N*). Please note the different scales used in (b) and (c). The shaded areas mark the surface mixed layers, for which the modeled rates should be treated with caution. Dashed lines are reference lines for zero modeled production/consumption rates. Due to the apparent intrusion of the more oxic Persian Gulf Water at St. 944 and upwelling at Sts. 946 and 949, which violate the assumptions of the applied model, modeled results for these latter stations are not shown here.

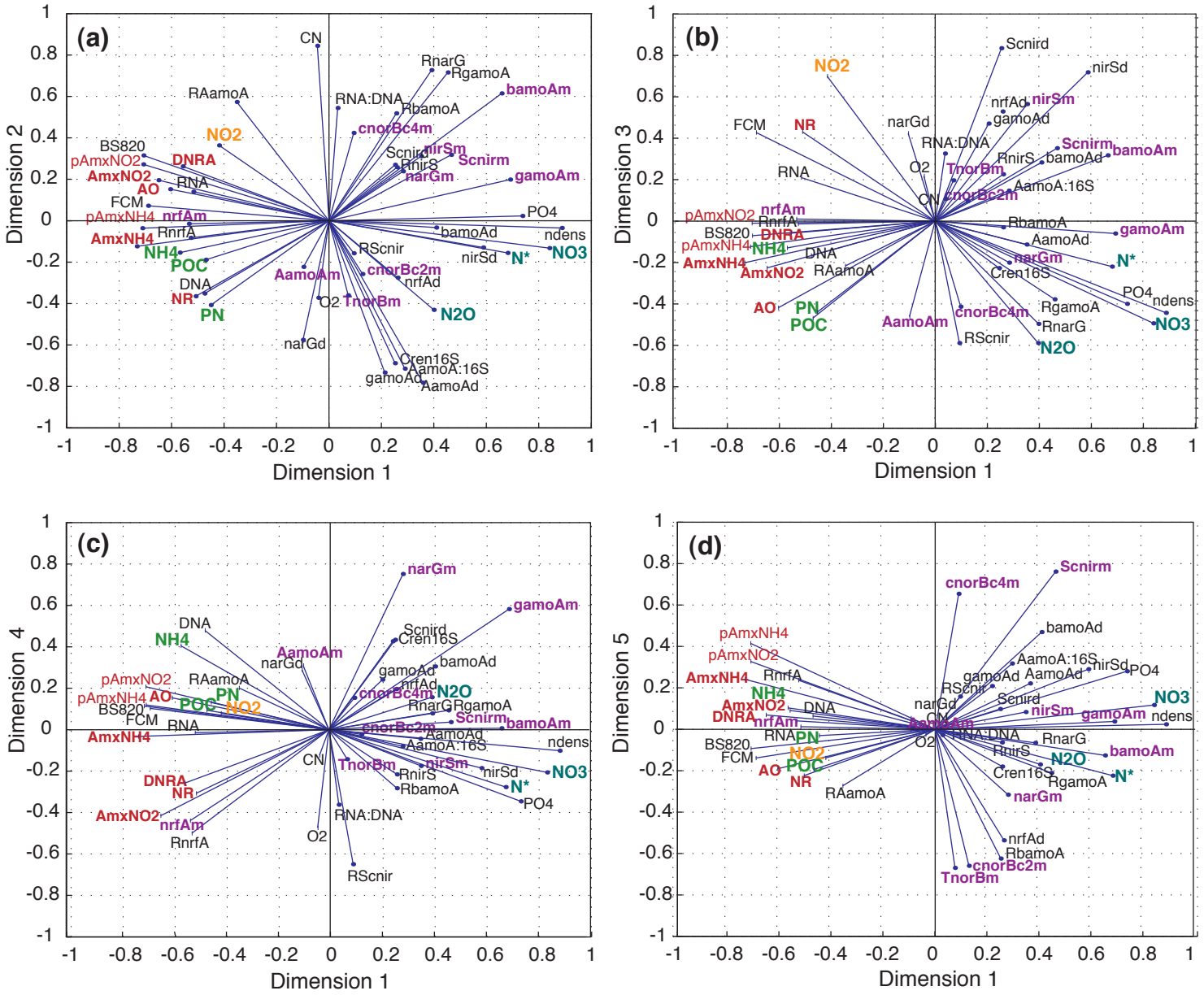

Figure A7. Non-metric multidimensional scaling analyses based on Spearman correlation of the various chemical and molecular parameters measured at all sampling stations in this study. Five dimensions were chosen with a final stress of 0.0633. Plotted above are the various measured parameters in the space of the resultant dimensions: (a) dimension 2 vs 1, (b) dimension 3 vs 1, (c) dimension 4 vs 1 and (d) dimension 5 vs 1. Apparent are especially the tight associations among the rates of various N-cycling processes (red), as well as their consistently close associations with ammonium and particulate organic matter (green). Only moderate and not always consistent relationship can be discerned between rates and nitrite (orange), while the latter seem to be associated with nitrate reduction (NR) and ammonia oxidation (AO). Most N-cycling rates show antagonistic relationships with nitrate, N*(in negative values) and nitrous oxide (dark cyan). Expression levels of various biomarker functional genes were marked in purple. Please refer to Table S2 for the abbreviations used for the variables analysed.

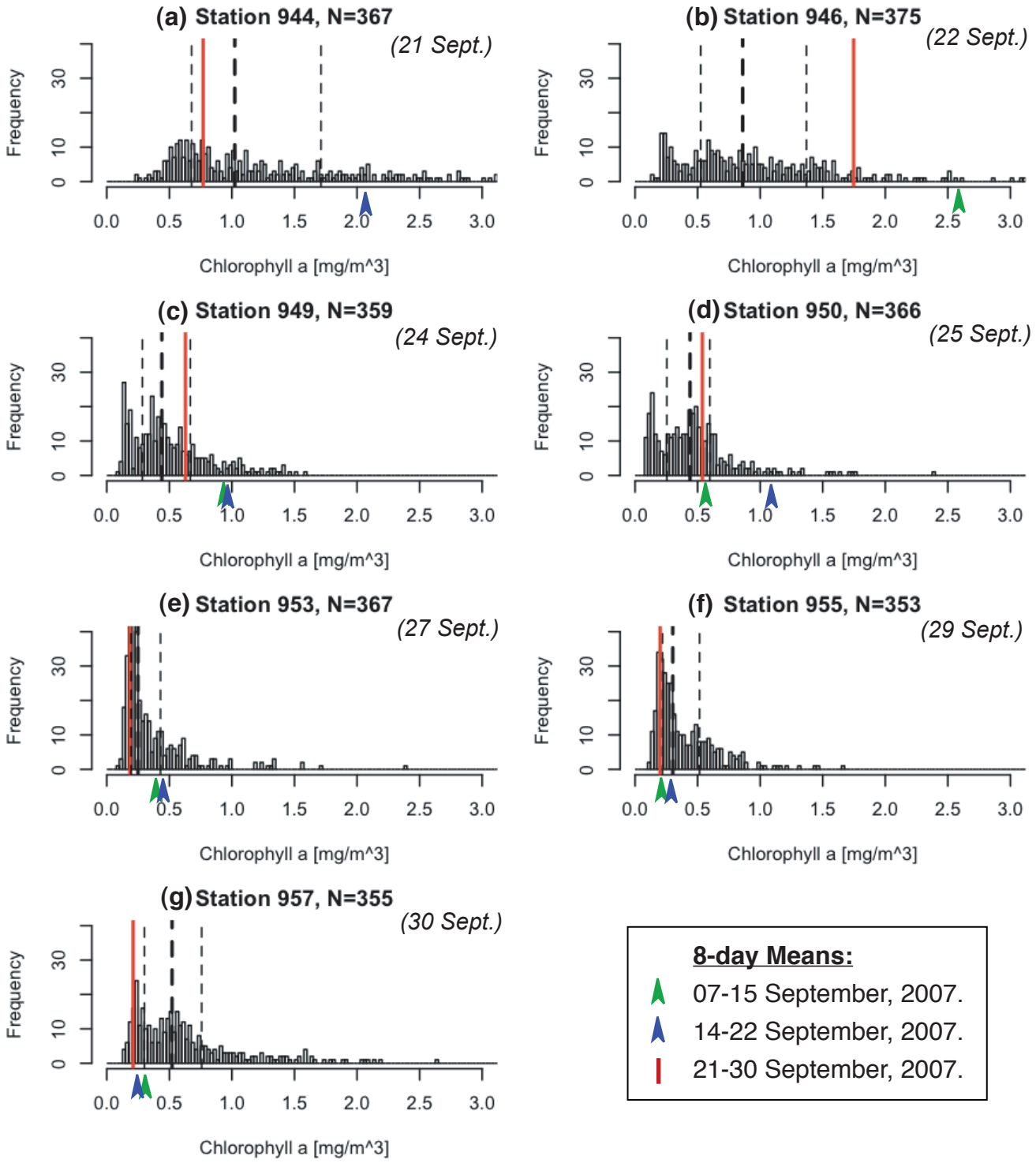

Figure A8. Histograms showing frequency distributions of surface chlorophyll *a* concentrations over a 10-year period (1998-2008) at the various sampling stations (averaged over 1°x1° grids), based on satellite data from Sea-viewing Wide Field-of-view Sensor (SeaWIFS): (a) St. 944, (b) St. 946, (c) St. 949, (d) St. 950, (e) St. 953, (f) St. 955 and (g) St. 957. The same scale for chl *a* is used for all stations. The thick dashed lines represent the median values for the respective stations, while the two thin dashed lines mark the upper and lower quartiles. Red lines show the 8-day mean surface chl *a* obtained in the week of sampling, and the exact sampling dates are shown in parentheses. The green and blue arrowheads indicate the 8-day means in the second and third weeks of September, 2007. As sinking organic matter takes time to travel from the surface to the underlying OMZ (starting at ~100 m depth), surface production during these 1-2 weeks before sampling may be more relevant to the microbial processes within the OMZ under investigation. Due to atmospheric interference (e.g. cloud cover, aerosols) particularly over the Omani Shelf, some 8-day means are unavailable for that region. Ocean color data used in this study were produced by the SeaWiFS Project at Goddard Space Flight Center. The data were obtained from the Goddard Earth Sciences Distributed Active Archive Center under the auspices of the National Aeronautics and Space Administration (NASA). Use of this data is in accord with the SeaWiFS Research Data Use Terms and Conditions Agreement.

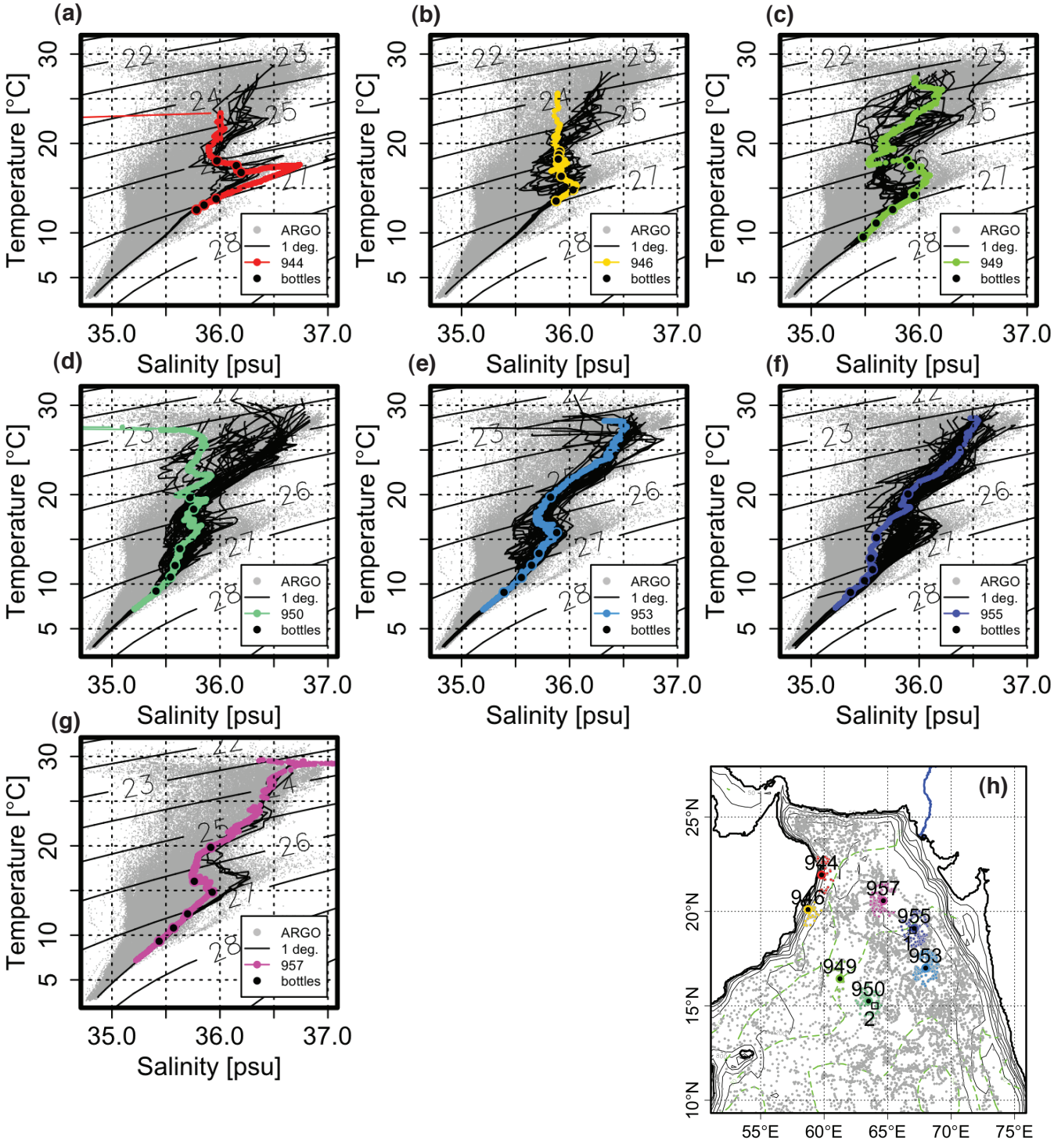

Figure A9. Temperature-salinity plots for the various sampling stations where ^{15}N-incubations were conducted in this study: (a) St. 944, (b) St. 946, (c) St. 949, (d) St. 950, (e) St. 953, (f) St. 955 and (g) St. 957. Coloured lines represent T-S relationships at the time of our sampling, whereas the black lines mark those obtained from Argo floats within 1 degree radii of the respective stations, and the grey dots show Argo data for the whole region as shown in the map (h). The corresponding isolines of potential density anomalies (kg m^{-3}) in the T-S space are also shown as thin black diagonals in (a) to (g). Black filled circles denote the depths where samples were collected for incubation experiments at each station. The Argos data were collected and made freely available by the International Argo Project and the national programs that contribute to it. (http://www.argo.ucsd.edu, http://argo.jcommops.org). Argo is a pilot program of the Global Ocean Observing System.